(21) Rosenke, K.; Zachmann, H. G. *Prog. Colloid Polym. Sci.* **1978**, *64*, 245.
(22) Schmeddig, P.; Zachmann, H. G. *Kolloid Z. Z. Polym.* **1972**, *250*, 1105.
(23) Helfand, E.; Wassermann, Z. R.; Weber, T. B.; Skolnick, J.; Runnels, J. R.; *J. Chem. Phys.* **1971**, *75*, 4441.
(24) Wefing, S.; Kaufmann, S.; Spiess, H. W. *J. Chem. Phys.* **1988**, *89*, 1234.
(25) Suter, U. W.; Neuenschwander, P. *Macromolecules* **1981**, *14*, 528.
(26) Theodorou, D. N. Ph.D. Thesis, MIT, 1985.
(27) Dannsso, F.; Moraglio, G. *Makromol. Chem.* **1958**, *28*, 250.
(28) Theodorou, D. N.; Ludovice, P. J.; Suter, U. W. In *Scattering, Deformation and Fracture in Polymers*; Wignall, G. D., Crist, B., Russell, T. P., Thomas, E. L., Eds.; *Material Research Society Symposia Proceedings* **1986**, *79*, 387.
(29) Samuels, R. J. *Structured Polymer Properties*; Wiley: New York, 1974.
(30) Natta, G. *Makromol. Chem.* **1960**, *35*, 94.
(31) Turner-Jones, A.; Aizlewood, J. M.; Beckett, D. R. *Makromol. Chem.* **1964**, *75*, 134.
(32) Addink, E. J.; Beintema, J. *J. Polym. Sci.* **1961**, *2*, 185.
(33) Mencik, Z. *J. Macromol. Sci.—Phys.* **1972**, *B6* (1), 101.
(34) Bunn, A.; Cudby, M. E. A.; Harris, R. K.; Packer, K. J.; Say, B. J. *Polymer* **1982**, *23*, 694.
(35) Gomez, M. A.; Tanaka, H.; Tonelli, A. E. *Polymer* **1987**, *28*, 2227.
(36) Wright, N. F.; Taylor, P. L. *Polymer* **1987**, *28*, 2004.
(37) Flocke, H. A. *Kolloid-Z.* **1962**, *180*, 118.
(38) McCrum, N. G. *Makromol. Chem.* **1959**, *34*, 50.
(39) Sauer, J. A.; Wall, R. A.; Fuschillo, N.; Woodward, A. E. *J. Appl. Phys.* **1958**, *29*, 1385.
(40) Krämer, H.; Helf, K.-E. *Kolloid-Z.* **1962**, *180*, 114.
(41) McBrierty, V. J.; Douglass, D. C.; Falcone, D. R. *J. Chem. Soc., Faraday Trans. 2* **1972**, *68*, 1051.
(42) Roy, S. K.; Kyu, T.; St. John Manley, R. *Macromolecules* **1988**, *21*, 499.
(43) McCall, D. W. *Natl. Bur. Stand. U.S. Spec. Publ.* **1969**, *301*, 475.
(44) States, D. J.; Haberkorn, R. A.; Ruben, D. J. *J. Magn. Reson.* **1982**, *48*, 286.
(45) Kaufmann, S.; Wefing, S.; Schaefer, D.; Spiess, H. W. *J. Chem. Phys.*, submitted.
(46) Williams, M. L.; Landel, R. F.; Ferry, J. D. *J. Am. Chem. Soc.* **1955**, *77*, 3701.
(47) Haward, R. N. *The Physics of Glassy Polymers*; Applied Science Publishers: London, 1973.
(48) Doolittle, A. K. *J. Appl. Phys.* **1951**, *22*, 1471; **1952**, *23*, 236.
(49) Dekmezian, A.; Axelson, D. E.; Dechter, J. J.; Borah, B.; Mandelkern, L. *J. Polym. Sci., Polym. Phys. Ed.* **1985**, *23* (2), 367.
(50) Fytas, G.; Ngai, K. L. *Macromolecules* **1988**, *21*, 804.
(51) Plazek, D. L.; Plazek, D. J. *Macromolecules* **1983**, *16*, 1469.
(52) Hagemeyer, A.; Schmidt-Rohr, K.; Spiess, H. W. *Adv. Magn. Reson.* **1989**, *13*, 85.
(53) Kawai, H.; Hashimoto, T.; Suehiro, S.; Fujita, K. *Polym. Eng. Sci.* **1984**, *24*, 361.

# Synthesis and Characterization of New Polymers Exhibiting Large Optical Nonlinearities. 1. Ladder Polymers from 3,6-Disubstituted 2,5-Dichloroquinone and Tetraaminobenzene

**Luping Yu and Larry R. Dalton***

*Department of Chemistry, University of Southern California,*
*Los Angeles, California 90089-0482*

*Received November 20, 1989; Revised Manuscript Received January 30, 1990*

ABSTRACT: Ladder polymers were synthesized from 3,6-disubstituted 2,5-dichloroquinones and tetraaminobenzene. The precursor to these polymers can be dissolved in organic solvents such as DMF, DMSO, and DMA. This solubility permits convenient processing of polymers into thin films which can subsequently be converted to fully fused-ring ladder polymers by thermal treatment. the final ladder polymers exhibited exceptional thermal stability (as determined by TGA) and laser damage thresholds in excess of 1 GW/cm$^2$. Degenerate four-wave-mixing measurements on these ladder polymers yielded third-order susceptibilities as high as $1.6 \times 10^{-9}$ esu, which is one of the highest values observed for an amorphous material.

Many organic and polymeric materials containing extended conjugated systems have been shown to exhibit large, ultrafast second- and third-order nonlinear optical susceptibilities.[1–3] A large number of potential applications, ranging from optical computing to sensor protection, exist for these materials. The most investigated polymer system is poly(diacetylene) (PDA), which has exhibited third-order susceptibilities as high as $8 \times 10^{-10}$ esu for single crystals;[3] however, amorphous PDA exhibits a much smaller $\chi^{(3)}$. If practical applications of polymers to the fabrication of nonlinear optical devices are to be pursued, then new polymer materials with much higher nonlinear optical susceptibilities, higher laser damage thresholds, improved optical transparency, and improved processibility must be developed. It is the search for such materials that motivates the present work.

Theory provides the direction for the development of new polymers. It is generally recognized that third-order susceptibility increases dramatically with $\pi$-electron delocalization.[4] Ladder polymers with the structure shown in Figure 1 not only possesses a conjugated $\pi$-electron system but the forced planarity of these polymers ensures optimum electron delocalization (the effectiveness of overlap of p orbitals is determined by $\theta$, the dihedral angle between p orbitals, through $\cos^2 \theta$). Theory predicts that even oligomers of these materials will exhibit significant third-order susceptibilities.[5] Scaling arguments would suggest significant increases in optical nonlinearity of polymers relative to the oligomeric compounds, although the increases would not be expected to continue indefinitely with polymer chain length due to self-localization effects (determined by intrinsic electron–phonon and electron–

0024-9297/90/2223-3439$02.50/0 © 1990 American Chemical Society

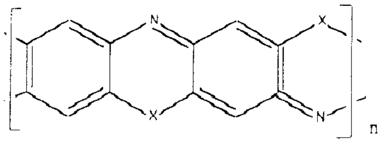

Where X = NH, O, S

**Figure 1.** Structure of ladder polymers.

coulomb interactions).[6]

Ladder polymers (see Figure 1) have been known for some time as materials that exhibit exceptional thermal stability and mechanical strength.[7] The major problem encountered with these materials is that of poor solubility, particularly in organic solvents. This intrinsic insolubility greatly inhibits characterization and the processing of these materials into forms other than powders. In fact, no one to date has ever made and unambiguously characterized a complete ladder polymer.[8] The insolubility of ladder polymers can reasonably be attributed to strong van der Waals interactions between the $\pi$-electron clouds of adjacent polymer chains and to the poor entropy of mixing associated with the rigid rod nature of the ladder polymers. It is reasonable that polymer–polymer interactions can be destabilized by introducing substituents and their associated steric interactions. Moreover, flexible-chain substituents are likely to improve the entropy of solution. The synthesis of ladder polymers via soluble flexible-chain precursor polymers should substantially improve processibility. Ideally, thin films could be prepared by using soluble precursor polymers, and then these films could be thermally processed into fully fused-ring ladder polymers. Such concepts have also been applied to the synthesis of other electroactive polymers including polythiophenes[9] and poly(*p*-phenylenevinylene).[10] In this paper, we report the synthesis of polyquinoline (PQL) type ladder polymers derivatized by (dialkylamino)vinyl substituents and their nonlinear optical property studies.

## Results and Discussion

Dichloroquinone monomers derivatized with various vinylamine substituents were prepared by reacting chloranil and acetaldehyde with diethylamine or piperidine in toluene at room temperature (see reaction Scheme I). As is evident from a consideration of the analytical data given in the Experimental Section, the monomers can be prepared in high purity; however, it is important to note that tetraaminobenzene (TAB) is quite sensitive to air oxidation. By careful control of oxygen exposure, we are able to prepare TAB with only 0.51% oxidation.

### Scheme I
### Preparation of Quinone Monomers

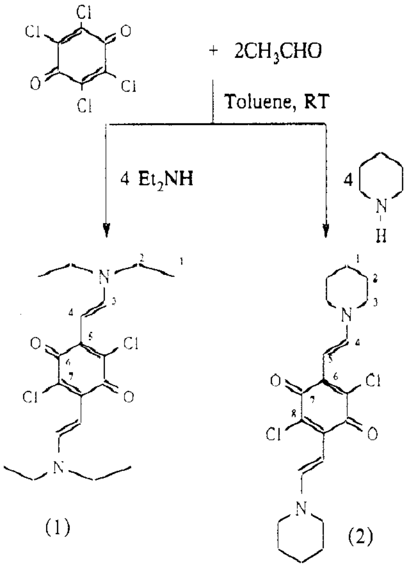

### Scheme II
### Polymerization between ((Dialkylamino)vinyl)dichloroquinone Monomers and TAB

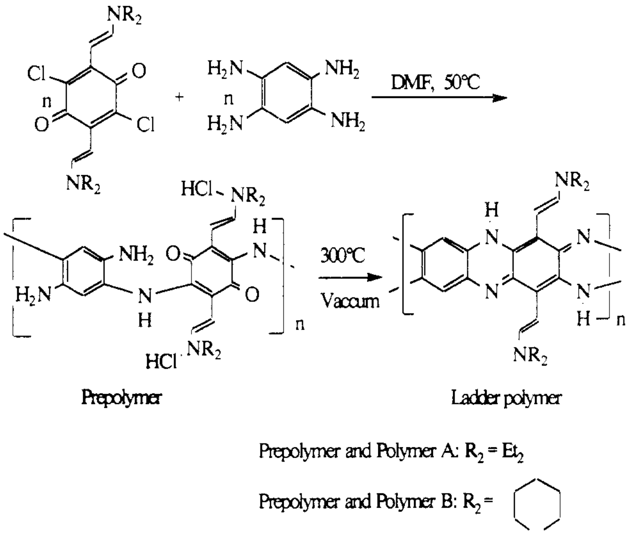

Quinone monomers 1 and 2 were used to synthesize prepolymers and polymers A and B, respectively. The synthesis of the ladder polymers involved two steps. First, the derivatized dichloroquinone monomers and TAB in DMF reacted at 50 °C to form a soluble open-chain polymer (hereafter referred to as "prepolymer"). The prepolymers were then heated in a vacuum oven to form polymer with ladder structure segments. The reaction of derivatized quinones with tetraaminobenzene is carried out in a glovebox filled with a helium atmosphere to avoid air oxidation. Polymerizations were attempted in a variety of solvents such as DMF, DMSO, DMAc, *m*-cresol, and pyridine. With *m*-cresol, it is very difficult to get rid of the solvent, and in pyridine the prepolymer exhibits poor solubility, precipitating out of solution as the polymerization reaction proceeds. The best solvents appear to be DMF and DMAc. We chose DMF as the solvent. The prepolymers were isolated from the reaction media by two different methods. DMF solutions were poured into chloroform and the precipitate was collected and dried under vacuum at 50 °C or DMF was removed by pumping on the prepolymer solution at ambient temperature until the weight became constant. To prepare films for optical measurements, the second procedure is preferred because after the prepolymer is precipitated from solution, it can only be partially redissolved in organic solvents.

Although structure elucidation is much more complex for polymers than for monomers, the following data from elemental analysis as well as NMR, FTIR, and UV–vis spectroscopy support the formation of the open-chain prepolymer in the first polymerization step shown in Scheme II.

Figure 2 shows the NMR spectra of quinone monomer 1 (curve 1) and prepolymer A (curve 2). The $^1H$ NMR spectrum of prepolymer A indicates some changes from that of quinone monomer 1. The chemical shift of methylene connected to nitrogen decreases from 3.35 to 2.88 ppm and that of the vinyl proton connected to nitrogen moves upfield from 5.50 to 5.80 ppm. One of the notable changes in the spectrum of the prepolymer is the

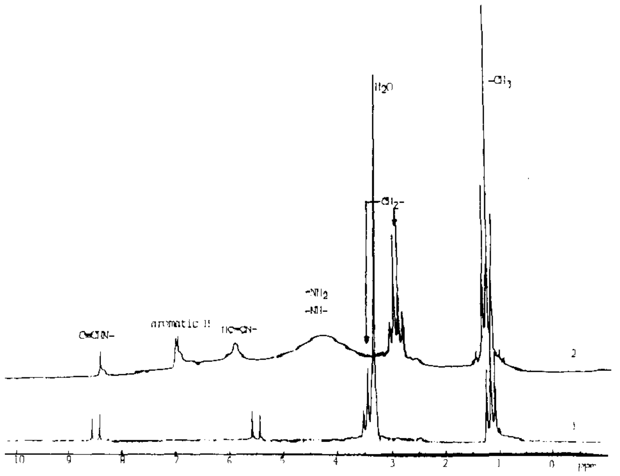

**Figure 2.** $^1H$ NMR spectra of (1) monomer 1 and (2) prepolymer A in DMSO-$d_6$.

**Table I**
**Tentative Assignment of FTIR Data for Prepolymer B and Ladder Polymer B**[a]

| absorp peaks of prepolymer, $cm^{-1}$ | remarks | absorp peaks of polymer, $cm^{-1}$ |
|---|---|---|
| 3370–3320 (s) | N–H, $H_2O$ associated with KBr | 3400 (s) |
| 2931–2850 (m) | $>CH_2$, str | 2930–2850 (w) |
| 1657 (s) | $>C=O$, str | disappears |
| | $>C=N-$, str | 1626 (s) |
| 1605 (w) | $>C=C<$, str | 1605 (w) |
| 1511 (s) | $-NH_2$, def | disappears |
| 1471 (m) | $-CH-$, $>CH_2$, def | 1471 (w) |
| 1435 (m) | H–C–H, scissoring | 1435 (w) |
| 1246 (s) | $>C-N-$, primary amine, str | very weak |
| 1184 (s) | aromatic C=C–H (1,2,4,5-substituted benzene in-plane def) | 1184 (m) |
| 1098 (s) | ? | disappears |
| 1029 (s) | C–C (skeletal vibrations in piperidine ring) | 1029 (w) |
| 947 (s) | C=C out-of-plane def | 947 (w) |
| 853 (s) | C–H out-of-plane bending, benzene | 974 (s) |
| 661 (m) | ? | very weak |
| 555 (m) | ? | disappears |

[a] References 11 and 12.

appearance of the $-NH-$ and $-NH_2$ chemical shifts in a broad overlapping band centered near 4.3 ppm. This is consistent with the presence of unreacted primary amine from TAB as well as the secondary $-NH-$ bond formed during polymerization. In addition, the chemical shift for the TAB aromatic protons can be seen.

A comparison of exemplary IR data of prepolymer B and ladder polymer B is given in Table I and will be discussed later. There are several features in the IR spectrum of the prepolymer that support the formation of the proposed structure (see Figure 3). Prepolymer B will be discussed, although similar features can be seen in the IR spectrum of prepolymer A. The amine peak below 3500 $cm^{-1}$ is too broad to assign definitely because of the overlap of bands for the primary amine, water from KBr pellets, and the secondary amine that forms part of the prepolymer backbone. The peak at 1511 $cm^{-1}$ can be assigned to the N–H bending of the primary amine, and the peak at 1471 can be assigned to N–H bending of the secondary amine.

Elemental analyses show very good agreement between experimental and theoretical results for the proposed prepolymer structures.

UV–vis spectra of the prepolymers are similar to each other (see curves 1 and 3 in Figure 4) but are quite different from the spectra of the quinone monomers (see curves 2 and 4). Low-energy absorption bands around 577 nm in the monomers disappear in the prepolymers in DMF solutions, indicating polymerization.

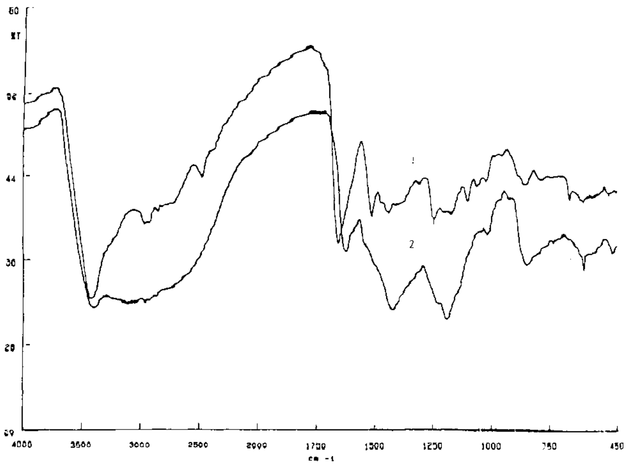

**Figure 3.** FTIR spectra of (1) prepolymer A and (2) ladder polymer A.

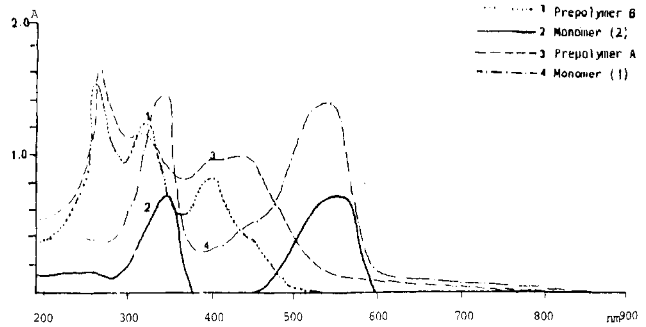

**Figure 4.** UV–vis spectra of (1) prepolymer B, (2) monomer 2, (3) prepolymer A, and (4) monomer 1 in DMF.

Viscosity measurements of the prepolymers in DMF at 25 °C gave 1.4 and 0.25 dL/g for prepolymers A and B, respectively, indicating a relatively low molecular weight for prepolymer B.

To make ladder polymers, films of the prepolymers were heated at 280–300 °C for 5 h. Elemental analysis indicates that the condensation did occur but one notes that it is very difficult to make a perfect ladder structure. Several events may accompany the second condensation: (1) the side groups may be driven off; (2) deamination may occur. All of these effects will make the ladder polymer imperfect. Elemental analysis results showed that the cleavage of side groups and deamination are of minor importance. The best fit structures of ladder polymers A and B based on elemental analysis results still have reasonably extended ladder structures (see Figure 5).

FTIR spectra (Figure 3) provide further evidence for the condensation between amine and carbonyl groups. From Figure 3 and Table I, several features can be extracted:

(1) In the prepolymer, we observe absorptions of $>C=O$ stretching (1657 $cm^{-1}$), $-NH_2$ out-of-plane deformation (1511 $cm^{-1}$), and $>C-N-$ stretching of the primary amine (1246 $cm^{-1}$). All these absorptions disappear or become greatly reduced after heating at 300 °C for 5 h.

(2) The vinyl out-of-plane deformation absorption at 947 $cm^{-1}$ and those related to the benzene ring still remain.

(3) A new strong band around 1626 $cm^{-1}$ appears, which can be assigned to $>C=N-$ stretching.

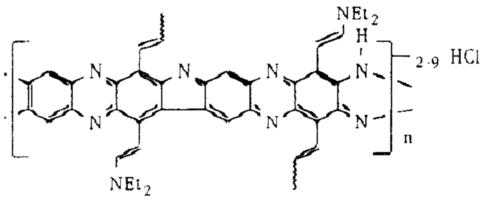

Best fit structure for polymer A

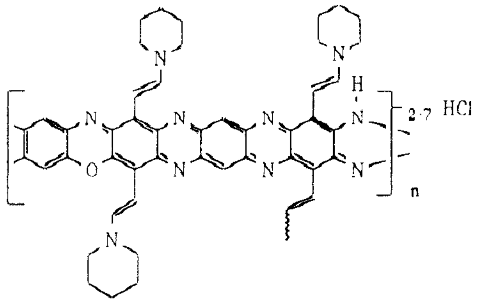

Best fit structure for polymer B

**Figure 5.** Best fit structures of polymers A and B.

**Table II**
**Solubilities (g/mL) of Prepolymer A and Polymer A**

| solvent | prepolymer A | polymer A |
|---|---|---|
| DMF | 0.010 | 0.000 |
| DMSO | 0.007 | 0.000 |
| DMA | 0.009 | 0.000 |
| *m*-cresol | 0.005 | 0.000 |
| HMPA | 0.001 | 0.000 |
| $CH_3SO_3H$ | 0.025 | 0.018 |
| $H_2SO_4$ | 0.025 | 0.022 |

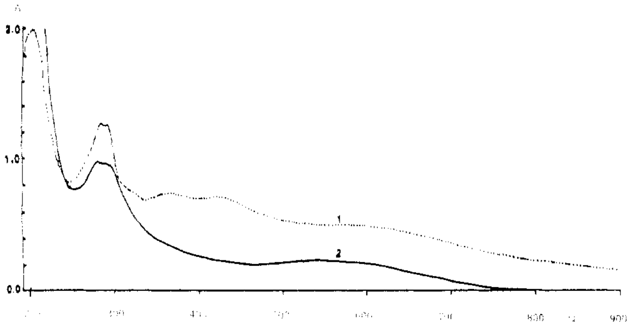

**Figure 6.** UV-vis spectra of (1) ladder polymer B and (2) prepolymer B in MSA.

(4) The peaks around 1500 and 1250 $cm^{-1}$ are broadened, which can be the effect of extended electron delocalization along the ladder structure.

Although derivatization improved the solubilities of prepolymers relative to underivatized prepolymers,[13] the van der Waals interactions in prepolymers and polymers are still strong enough to limit the solubility of both. Table II gives the results of solubility measurements of prepolymer A and polymer A. It was found that once a prepolymer precipitated out of solution, it could only be partially redissolved in organic solvents.

UV-vis spectra of both prepolymer B and polymer B in methanesulfonic acid (MSA) show different structures (see Figure 6). The spectrum of polymer B in MSA shows a lower $\pi$-$\pi^*$ band energy edge at 795 nm when compared with that of prepolymer B at 693 nm, which implied that the polymer system has a more extended $\pi$-electron conjugation system. One may note that the UV-vis spectrum of prepolymer B in methanesulfonic acid shows a different feature from that in DMF solution. An extra low-energy peak at 693 nm appeared in this former spectrum, which is not observed in spectra of either the amine or quinone monomer **2** in MSA media. This feature may imply that MSA promotes condensation between amine and carbonyl groups. These UV-vis spectral features were identical with those of prepolymer A and polymer A.

**Table III**
**TGA Decomposition Temperature (°C) of Ladder Polymers**[a]

| sample | prepolymer[b] | polymer |
|---|---|---|
| A | 620 | 690 |
| B | 470 | 474 |

[a] Decomposition temperatures are deduced as shown in Figure 7. [b] Temperature of second stage of weight loss of prepolymers.

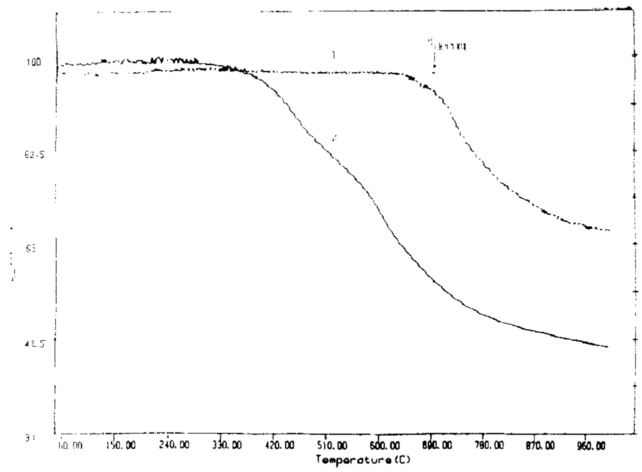

**Figure 7.** TGA diagrams of (1) ladder polymer A and (2) prepolymer A. Heating rate: 20 °C/min.

**Table IV**
**ESR Measurements of Ladder Polymers**

| | prepolymer | | polymer | |
|---|---|---|---|---|
| parameter | A | B | A | B |
| $\Delta H$ (G) | 9.00 | 10.05 | 6.30 | 7.50 |
| *g* | 2.00515 | 2.00510 | 2.0034 | 2.00312 |

TGA of these polymers indicates high thermal stabilities. Table III summarizes the decomposition temperatures of ladder polymers under a nitrogen atmosphere. Polymer A exhibits a higher thermal stability than polymer B, which might indicate that polymer B is less perfect in ladder structure than polymer A. TGA is a good indicator for solid-state reactions. For instance, several features can be noted from the TGA diagram of prepolymer A (see Figure 7). First, weight loss which might involve a condensation reaction between carbonyl groups and amino groups as well as elimination of hydrogen chloride starts at ca. 300–330 °C. The second stage of weight loss appears at ca. 580 °C for prepolymer A. This is consistent with the first weight loss in the TGA diagram of polymer A which is condensed from prepolymer A by heating at 300 °C (see Table III). This feature can be attributed to cleavage of side groups and degradation of the main chain. The high thermal stability of these polymers gives rise to a high laser damage threshold, which has been demonstrated in degenerate four-wave-mixing (DFWM) measurements. Laser damage thresholds greater than 1 GW/$cm^2$ have been observed for both ladder polymers.

Both prepolymers and polymers in the solid state are ESR active. Table IV lists the ESR results of the prepolymers and polymers. In the prepolymers, *g* values significantly shift from that of the free-electron value (2.0023), as might be expected for quinone radicals. The *g* values

Table V
Optical Properties of Ladder Polymers

| property[a] | polymer sample A | polymer sample B |
|---|---|---|
| $n$ | 1.96 ± 0.02 | 1.92 ± 0.02 |
| $\alpha$, $\mu m^{-1}$ | 2.32 ± 0.16 | 1.88 ± 0.31 |
| $\chi^{(3)}{}_{1111}$, $\times 10^{-10}$ esu | 9.78 ± 3.0 | 7.40 ± 2.1 |
| $\chi^{(3)}{}_{1221}$, $\times 10^{-10}$ esu | 1.8 ± 0.5 | 1.6 ± 0.5 |
| $\chi^{(3)}{}_{T}$, $\times 10^{-10}$ esu | 3.8 ± 1.2 | 3.8 ± 1.2 |
| $\chi^{(3)}{}_{1111}/\alpha$, $\times 10^{-10}$ esu $\mu m$ | 3.23 | 3.93 |

[a] $n$ is the index of refraction; $\alpha$ is the absorption coefficient; $\chi^{(3)}$ is the third-order susceptibility; $\chi^{(3)}{}_{ijk}$'s are the tensorial components of the third-order susceptibilities; $\chi^{(3)}{}_{T}$'s are the thermal contributions to the third-order NLO processes.

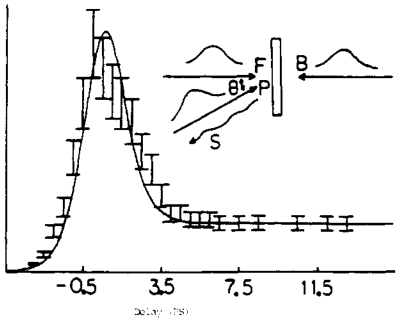

Figure 8. DFWM signal of ladder polymer B. The signal amplitude is in arbitrary units.

Table VI
Effects of Oxidation and Cyclization

| property | polymer A | polymer A (oxidized) | prepolymer A |
|---|---|---|---|
| $n$ | 1.96 | 1.75 | 1.70 |
| $\alpha$, $\mu m^{-1}$ | 2.32 | 1.10 | 1.70 |
| $\chi^{(3)}{}_{1111}$, $\times 10^{-10}$ esu | 9.78 | 0.60 | 1.00 |
| $\chi^{(3)}{}_{1111}/\alpha$, $\times 10^{-10}$ esu $\mu m$ | 3.23 | 0.54 | 0.59 |

of the polymers are identical with those of underivatized ladder polymers and are near the free-electron value, implying significant electron delocalization.[6] Line-width changes from prepolymer to polymer also imply a greater electron delocalization in the latter.

Table V presents the linear and nonlinear optical (NLO) properties of the polymers. The data in Table V demonstrate that $\chi^{(3)}$ values of these polymers are very high. As an example, Figure 8 shows a typical plot of DFWM signal pulse energy versus the delay time (both plus and minus) of the forward pump beam F for polymer B; each data point is an average over 10–20 pulse energy fluctuations on the order of 20%. In this figure, all polarizations are horizontal and both fast and slow components are clearly visible. From Figure 8, we can see that electronic NLO processes in this polymer system are ultrafast processes with response times less than the laser limit resolution. From a practical point of view, the value of $\chi^{(3)}/\alpha$ has more important meaning than that of $\chi^{(3)}$, which is a characteristic value of the material. The results in Table V show that these polymers have very high $\chi^{(3)}/\alpha$ values. Both of these materials exhibit identical results, which implies that different alkyl substituents on the amine have only a minor influence on the NLO properties as long as we maintain the ladder structure with aminovinyl derivatization. It was found that the oxidation of a sample will reduce the nonlinearity by reducing electron localization (see Table VI). The NLO results reported here are consistent with a dependence of third-order susceptibility upon electron delocalization length with the clear indication that polymer imperfections limit delocalization length for many preparations. The results are also consistent with an important resonant contribution to optical nonlinearity as susceptibilities follow optical absorptions.

## Experimental Section

All reagents and solvents were of analytical grade quality, purchased commercially from Aldrich Chemical Co. and used without further purification unless otherwise noted. DMF was purified by distillation from $P_2O_5$. The melting points were obtained with open capillary tubes on a Mel-Temp apparatus and are uncorrected. Polymerization was carried out in a Vacuum Atmospheres Corp. helium-filled glovebox.

**Synthesis and Characterization of Monomers. 2,5-Dichloro-3,6-bis(2-(diethylamino)vinyl)benzoquinone (1).** This compound was synthesized by an improved literature procedure.[14] Diethylamine (2.9 g, 0.04 mol) was added to a stirred solution of chloranil (4.92 g, 0.02 mol) and freshly distilled acetaldehyde (1.80 g, 0.04 mol) in toluene (1500 mL) at 60 °C. A blue solution was formed within 10 min, and more diethylamine (2.9 g, 0.04 mol) was added to the solution. After 5 h, 0.5 N sulfuric acid was added to extract amine salts, and the toluene layer was separated from the aqueous layer, dried over 3-Å molecular sieves, and concentrated by evaporation. The product was purified by chromatographic separation using deactivated alumina (which is prepared by adding a specific amount of water) with toluene/methylene chloride as flow solvent. The final yield is 51.2% (mp 129–131 °C). $^1H$ NMR ($CDCl_3$) $\delta$ 1.2 (t, 12 H, $CH_3$, $J$ = 9.9 Hz), 3.4 (q, 8 H, $CH_2$, $J$ = 9.9 Hz), 5.6 (d, 2 H, HC=CN, $J$ = 12.6 Hz), 8.5 (d, 2 H, =CHN, $J$ = 12.6 Hz). $^{13}C$ NMR ($CDCl_3$) $\delta$ 12.0 ($C_1$), 14.0 ($C_{1'}$), 42.0 ($C_2$), 51.0 ($C_{2'}$), 94.5 ($C_4$), 119.0 ($C_5$), 139.5 ($C_6$), 153.0 ($C_3$), 178.6 ($C_7$).

Anal. Calcd for $C_{18}H_{24}N_2C_{12}O_2$: C, 58.22; H, 6.47; N, 7.55; Cl, 19.14. Found: C, 58.30; H, 6.53; N, 7.52; Cl, 19.16.

**2,5-Dichloro-3,6-bis(2-piperidinovinyl)benzoquinone (2).** Chloranil (4.92 g, 0.02 mol) and acetaldehyde (1.80 g, 0.04 mol) were added to toluene (1400 mL) and stirred for 5 min. To this solution was added dropwise piperidine (3.44 g, 0.04 mol). The solution was blue after 10 min of stirring, and more piperidine (3.44 g, 0.04 mol) was then added to this blue solution, which changed gradually to purple. The reaction was stirred at 30 °C for 7 h and then quenched by addition of 0.5 N sulfuric acid, which also served to extract amine salts. The toluene layer was washed with water and dried over 3-Å molecular sieves. The solution was concentrated by evaporation to ca. 60 mL. Needle crystals were collected by suction and then washed with a small portion of cold toluene. The product was recrystallized from toluene, giving the final product (1.5 g, 4.1 mmol, 21% yield) with mp 180–182 °C. $^1H$ NMR ($CDCl_3$) $\delta$ 1.65 (s, 12 H, $CH_2$), 3.35 (s, 8 H, $CH_2$), 5.65 (d, 2 H, HC=C, $J$ = 12.6 Hz), 8.50 (d, 2 H, =CHN, $J$ = 12.6 Hz). $^{13}C$ NMR ($CDCl_3$) $\delta$ 26.5 ($C_1$), 28.5 ($C_2$, $C_{2'}$), 47.0–56.0 ($C_3$, $C_{3'}$), 96.5 ($C_5$), 123.0 ($C_6$), 144.0 ($C_7$), 155.5 ($C_4$), 180.0 ($C_8$).

Anal. Calcd for $C_{20}H_{24}N_2O_2Cl_2$: C, 60.76; H, 6.08; N, 7.09; Cl, 17.97. Found: C, 60.83; H, 6.18; N, 7.06; Cl, 17.89.

**1,2,4,5-Tetraaminobenzene (TAB).** TAB was prepared as previously described.[16] 1,2,4,5-Tetraaminobenzene tetrahydrochloride was made by reduction of 2,4-dinitro-1,5-diaminobenzene using stannous chloride dihydrate in concentrated hydrochloric acid.[15,16] To remove trace amounts of tin ions in the final product, $H_2S$ was bubbled through the TAB·4HCl solution. The free amine was made following Vogel's procedure.[17] White flat crystals with mp 272–274 °C were obtained, which is consistent with the literature result (mp 274–276 °C).[17]

Anal. Calcd for $C_6H_{10}N_4$: C, 52.17; H, 7.24; N, 40.58; O, 0.00. Found: C, 52.11; H, 7.09; N, 40.31; O, 0.51.

**Synthesis and Characterization of Polymers. Prepolymer A from TAB and 1.** To DMF (100 mL) were added compound 1 (5.0 g, 0.015 mol) and TAB (1.855 g, 0.015 mol). The resulting solution was stirred at room temperature overnight. The brown solution obtained can immediately be used to cast films on glass plates. To remove trace amounts of unreacted starting material, the solution was poured into chloroform (500 mL). The precipitate was collected by filtration and washed with chloroform and ethanol. The dark brown prepolymer was dried at 50 °C under vacuum (95% yield). FTIR (KBr pellets)

3246 (NH, $H_2O$), 2975 ($CH_2$, $CH_3$, stretch), 1656 (C=O, stretch), 1511 (NH, deformation), 1438 ($CH_2$, scissoring), 1244 (CN, stretch of primary amine), 1170 (1,2,4,5-substituted benzene in-plane deformation), 976 (C=, out-of-plane deformation), 855 $cm^{-1}$ (CH, out-of-plane bending of benzene ring). $^1H$ NMR (DMSO-$d_6$) $\delta$ 1.2 (t, 12 H, $CH_3$, $J$ = 9.9 Hz), 2.9 (8 H, $CH_2$, $J$ = 9.9 Hz), 3.8 (s, $NH_2$), 5.85 (d, 2 H, =CHN, $J$ = 12.0 Hz), 6.8–7.0 (aromatic H), 8.4 (s, 2 H, HC=CN).

Anal. Calcd for $(C_{24}H_{34}N_6Cl_2O_2)_n$: C, 56.58; H, 6.68; N, 16.50; Cl, 13.95. Found: C, 56.89; H, 6.45; N, 16.69; Cl, 13.71.

**Polymer A (Ladder Type).** Polymer A can be made by two ways: (a) By reflux of the prepolymer solution in DMF overnight, a black powder was precipitated out and collected by filtration. The powder was extracted with ethanol in a Sohxlet extractor and dried at 100 °C under vacuum (90% yield). (b) The polymer can also be obtained by heating the prepolymer film or powder at 140 °C for 6 h and at 300 °C for 10 h. FTIR spectra showed that these two procedures give the same polymers. FTIR (in KBr) 3388 (NH, $H_2O$), 2975 ($CH_2$, $CH_3$, stretch), 1621 (C=N, stretch), 1191 (1,2,4,5-substituted benzene in-plane deformation), 976 (C=C, out-of-plane deformation), 847 $cm^{-1}$ (C–H, out-of-plane bending of benzene ring).

Anal. Calcd for $(C_{24}H_{30}N_6Cl_2)_n$: C, 60.88; H, 6.34; N, 17.75; Cl, 15.01. Found: C, 65.13; H, 4.49; N, 16.70; Cl, 13.97. Best fit structure $(C_{40}H_{34}N_9Cl_{2.9})_n$: C, 64.60; H, 4.57; N, 16.95; Cl, 13.85.

**Prepolymer B.** Prepolymer B was synthesized as for prepolymer A from compound **2** and TAB. $^1H$ NMR (DMSO-$d_6$) 1.41 (s, 12 H, $C^1H_2$), 2.80 (s, 8 H, $C^{2,3}H_2$), 4.2 (s, $NH_2$), 5.78 (s, 2 H, =CHN), 6.5–6.9 (s, aromatic H), 8.35 (s, 2 H, HC=CN). FTIR (in KBr) results are listed in Table I.

Anal. Calcd for $(C_{26}H_{34}N_6Cl_2O_2)_n$: C, 58.53; H, 6.38; N, 15.75; Cl, 13.32. Found: C, 58.03; H, 5.73; N, 16.41; Cl, 13.12.

**Polymer B.** Polymer B was synthesized from prepolymer B: FTIR (KBr) results are listed in Table I.

Anal. Calcd for $(C_{26}H_{30}N_6Cl_2)_n$: C, 62.76; H, 6.03; N, 16.90; Cl, 14.28. Found: C, 65.11; H, 5.58; N, 16.49; Cl, 10.92. Best fit structure $(C_{47}H_{46}N_{10}Cl_{2.7}O)_n$: C, 65.44; H, 5.44; N, 16.24; Cl, 11.12.

**Characterization.** FTIR spectra of polymers were obtained as potassium bromide pellets or polymer films on a 1760 Perkin-Elmer FTIR spectrometer. UV–vis spectra of the prepolymers were obtained in DMF or in methanesulfonic acid (MSA), and those of the polymers were obtained in MSA or as films on a Perkin-Elmer Lambda 4c UV–vis spectrophotometer. Thermal gravimetric analysis was performed with a Perkin-Elmer TGA 7 thermal gravimetric analyzer. NMR spectra were recorded on a JEOL FX 90Q FTNMR spectrometer. EPR measurements were carried out on an IBM ER 200D-SRC ESR spectrometer. To get accurate $g$ values, a $^{15}N$-PD-tempone in a toluene-$d_8$ sample with a known $g$ value (2.00602 ± 0.00005) was used as a standard. Intrinsic viscosities of the prepolymers were obtained in DMF at 25 °C.

The solubilities of the polymers were determined by stirring a known quantity of the polymer (0.25 g) in 10 mL of solvent for 48 h. At the conclusion, the solution was filtered and the undissolved portion of polymer was collected, washed with ethanol and then water, and dried at 50 °C in a vacuum oven. The solubility was calculated based on the weight of residue.

NLO measurements were performed by using a degenerate four-wave-mixing (DFWM) technique. Before we discuss measurements of third-order susceptibilities, it is important to consider ancillary measurements. Refractive indices were obtained by measuring back-reflection from the polymer–air interface at the operating wavelength for third-order susceptibility measurements (typically 532 nm). The reflection could be measured with an accuracy of better than 3%. Film thicknesses were measured with a step profiler (Tencor Instruments Alpha Step Profiler Model 1000) and were verified by electron microscopy. Film thickness varied from 0.4 to 4.0 μm. Hellwarth and co-workers[17] have introduced a new variation of the degenerate four-wave-mixing technique that permits measurement of all tensor components, $\chi_{ijkl}$, of the fast component of $\chi^{(3)}$, as well as of the slow component which gives the acoustic velocity and damping coefficients. A "phase conjugation" geometry for DFWM is employed in which all four beam polarizations can be varied to give independent data. Three input beams are formed from 532-nm laser pulses (derived from 5-Hz repetition rate mode-locked pulses from a Quantel Model YG471-C Nd:YAG laser which has been frequency doubled to 532 nm) having a pulse width of approximately 25 ps. In this geometry, delaying each of the three input beam pulses separately also gives three different and independent sets of data for the strength and polarization of the fourth signal beam. The three input beams (see Figure 8) are denoted "F" for the forward beam, "B" for the backward pump beam, and "P" for the probe beam (which impinges on the sample at a variable angle of ca. 10–20° to beam F). We have performed experiments with essentially all combinations of beam polarization and delay. A detailed discussion of this effort will be presented elsewhere.[17]

**Acknowledgment.** We thank Dr. R. W. Hellwarth, Mr. X. F. Cao, and Mr. J. P. Jiang from the Physics Department of the University of Southern California for DFWM measurements and Dr. R. Vac for proofreading and helpful discussion. This work was supported by Air Force Office of Scientific Research Contracts F49620-87-C-0100 and F49620-88-C-0071.

## References and Notes

(1) Chemla, D. S.; Zyss, J., Eds. *Nonlinear Optical Properties of Organic Molecules and Crystals*; Academic Press: New York, 1987; Vol. 1, 2.

(2) Williams, D. J., Ed. *Nonlinear Optical Properties of Organic and Polymeric Materials*; ACS Symposium Series 233; American Chemical Society: Washington, DC, 1983.

(3) Hermann, J. P.; Smith, P. W. *Dig. Tech. Pap.—Int. Quantum Electron. Conf., 11th* **1980**, 656.

(4) Agrawal, G. P.; Cojan, C.; Flytzanis, C. *Phys. Rev.* **1978**, *B17*, 776.

(5) (a) Boudreaux, D. S.; Chance, R. R.; Wolf, J. F.; Shacklette, L. W.; Bredas, J. L.; Themans, B.; Andre, J. M.; Silbey, R. *J. Chem. Phys.* **1986**, *85*, 4584. (b) de Martino, R., private communication. Unpublished computations from Hoechst Celanese, for example, give $\gamma$ values of aminonitro-substituted triphenodioxazine of (24.8–64.3) × $10^{-35}$ esu, depending on the position of the nitro substituent.

(6) Dalton, L. R.; Thomson, J.; Nalwa, H. S. *Polymer* **1987**, *28*, 543.

(7) Stille, J. K.; Mainen, E. L. *Macromolecules* **1968**, *1*, 36.

(8) Yu, L. P.; Chen, M.; Dalton, L. R. "Review of Ladder Polymers", in preparation.

(9) Bryce, M. R.; Chissel, A.; Kathirgamanathan, P.; Parker, D.; Smith, N. R. M. *J. Chem. Soc., Chem. Commun.* **1987**, 466.

(10) Wnek, G. E.; Chien, J. C. W.; Karasz, F. E.; Lillya, C. P. *Polymer* **1979**, *20*, 1441.

(11) Socrates, G. *Infrared Characteristic Group Frequencies*; Wiley: New York, 1975.

(12) Pretsch, E.; Seibl, J.; Simon, W.; Clerc, T. *Tables of Spectra Data for Structure Determination of Organic Compounds*; Springer-Verlag: Berlin, 1983.

(13) (a) Berlin, A. A.; Matreeva, Nn. G. *Vysokomol. Soedin.* **1959**, *1*, 1643. (b) Lindsey, A. S. In *The Chemistry of Quinoid Compounds*; John Wiley & Sons: New York, 1974; Part 2, Chapter 15, p 793.

(14) Buckley, D.; Henbest, H. B.; Slade, P. *J. Chem. Soc.* **1957**, 4891.

(15) Nietzki, R.; Schedler, A. *Ber.* **1897**, *30*, 1666.

(16) Vogel, H. A.; Marvel, C. S. *J. Polym. Sci.* **1961**, *50*, 511.

(17) Cao, X. F.; Jiang, J. P.; Bloch, D. F.; Hellwarth, R. W.; Yu, L. P.; Dalton, L. R. *J. Appl. Phys.* **1989**, *65*, 5012.